

**Hanna WRZESIŃSKA<sup>1)</sup>, Zygmunt RYMUZA<sup>2)</sup>, Karolina MAŁYSKA<sup>2)</sup>**  
Institute of Electron Technology<sup>1)</sup>  
Warsaw University of Technology, Institute of Micromechanics and Photonics<sup>2)</sup>

## **NANOMECHANICAL BEHAVIOUR OF ULTRATHIN NITRIDE FILMS DEPOSITED ON SILICON**

### **Key words**

Nanoindentation, ultrathin films, nitride films, microelectronic dielectric films.

### **Słowa kluczowe**

Nanoindentacja, warstwy ultracienkie, warstwy azotkowe, mikroelektroniczne warstwy dielektryczne.

### **Summary**

Nanoindentation tests were performed for TiN, CrN, NbN ultrathin films deposited on single crystal silicon wafer to estimate their hardness and elasticity modulus. The results of the investigation were compared with the same studies carried out for the microelectronic dielectric films SiO<sub>2</sub> (two types - thermally and plasma deposited) and Si<sub>3</sub>N<sub>4</sub>. The demonstrated better mechanical properties of the first group of the films predestinate them to be used as protective films in Micro Electro Mechanical System (MEMS) devices.

### **INTRODUCTION**

Ultrathin films are interesting coatings to perform mechanical and tribological functions in magnetic recording technology, micro electromechanical systems (MEMS) and atomic force microscopy (AFM) [1-4]. In such applications typical thickness of the film is as small as 10-200 nm only. There is a need for hard and wear-resistant films to protect the underlayer materials of components against wear. The wear resistance is usually correlated with good mechanical properties [5-8]. To shorten the tests time in the first preliminary study before tribological tests, the mechanical tests are very effective also looking for the level of coats. The selection of films with good nanomechanical behaviour is therefore of great interest for further tribological tests of the discussed ultrathin films.

The selection of the material for the protective films is not easy task. Some previous studies [9-14] have shown that the nitride films demonstrated good mechanical and tribological properties. These results are related, however, to relatively thick films (2-10  $\mu\text{m}$ ). It was interesting for us to test nitride ultrathin films for seen the above mentioned possible applications. The results of the investigation of such films would be useful not only to apply them directly in microengineering of protective coatings but also by estimation of the nanomechanical properties in modelling of mechanical behaviour of multilayer coatings composed of many thin layers composed of different materials [15-18].

## EXPERIMENTAL DETAILS

The following materials were selected to be used in deposition of the ultrathin films : TiN, CrN and NbN. The n-type <100> single crystal silicon was used as substrate material. The substrate was typical silicon wafer applied in microelectronics technology what is particularly important in the case of the application of the results of tests directly in the construction MEMS devices. For the comparison typical films used in microelectronics composed of silicon dioxide or silicon nitride were also studied.

The TiN, CrN, NbN films were deposited by reactive magnetron sputtering (Physical Vapour Deposition – PVD process) using Leybold's L400 Sp system. The deposition was performed without rotation of the table. The initial pressure in the chamber was held  $p_0 < 2 \times 10^{-6}$  mbar and the argon pressure  $p_{Ar} = 2,8 \times 10^{-3}$  mbar. The pressure of nitrogen was  $p_N = 3,8 \times 10^{-4}$  mbar. The power of the supply system was kept on 0.4 kW level. The rates of the deposition were following: TiN – 0.65 nm/s, CrN – 1.5 nm/s, NbN – 0.825 nm/s. The thickness of the produced films measured by ellipsometry was 195, 225, 165 nm respectively for TiN, CrN and NbN films.

The  $\text{SiO}_2$ ,  $\text{Si}_3\text{N}_4$  films were deposited by low temperature plasma chemical vapour (PECVD) technique using Oxford's PlasmaLab100 system. The following conditions were kept during the deposition process:  $T = 300^\circ\text{C}$ ,  $p = 1\text{Tr}$ , generator 13,56 MHz, power of the generator  $P=16\text{W}$ , gas flows for  $\text{SiO}_2$ :  $\text{SiH}_4/\text{N}_2 - 1125 \text{ cm}^3/\text{min}$ ,  $\text{N}_2\text{O} - 750 \text{ cm}^3/\text{min}$ , for  $\text{Si}_3\text{N}_4$ :  $\text{SiH}_4/\text{N}_2 - 1000 \text{ cm}^3/\text{min}$ ,  $\text{NH}_3 - 20 \text{ cm}^3/\text{min}$ . The time of deposition was 4 min for  $\text{SiO}_2$  and 16 min for  $\text{Si}_3\text{N}_4$ . The thickness of the films was 200 nm. The  $\text{SiO}_2$  film was also manufactured in typical thermal process used in microelectronics technology. The process was done in quartz tube of the diffusion furnace manufactured by Przemysłowy Instytut Elektroniki (PIE) Poland at temperature  $T=1000^\circ\text{C}$  by dry/wet/dry process (i.e. dry oxidation in oxygen atmosphere, wet oxidation in the water vapour atmosphere produced by hydrogen and oxygen synthesis). The procedure during the thermal oxidation was as follows: I phase (dry oxidation):

O<sub>2</sub> – 2.5 l/min, t=10 min, II phase (wet oxidation): O<sub>2</sub> –2.5 l/min, H<sub>2</sub> – 4.2 l/min, t=25 min, III phase (dry oxidation): O<sub>2</sub> – 2.5 l/min, t=10 min.

The nanoindentation was used to perform the nanomechanical tests. A special system called TriboScope (Hysitron Inc.) combined with Atomic Force Microscope (AFM) was applied to carry out the experiments. A Berkovich's diamond indenter [2, 16] was used for all indentations made during the tests. For all samples, a triangular load function consisting of a 5 second loading segment and a 5 seconds unloading segment with a maximum normal load obtained during experiment. It was important to make indents which depth were about 10% of coating thickness to avoid the effect of the substrate on the mechanical properties measured for the film [2, 19]. The result was that a contact depth was around 20 nm.

The maximum load was 500 μN applied in the case of NbN, CrN and TiN films was 500 μN and 350-450 μN for SiO<sub>2</sub>, Si<sub>3</sub>N<sub>4</sub> films.

In indentation mode, the instrument is a load-controlled displacement-sensing device. An indenter tip is driven into a sample and then withdrawn by decreasing the applied force. The applied load (P) and depth of penetration (h) into the sample are continuously monitored. A load versus displacement (depth) (L-D) curve can then be generated from the collected data. Figure 1 depicts an example of a load vs. depth curve. The sample hardness (H) and reduced elasticity modulus (E<sub>r</sub>) can then be calculated from the curve.

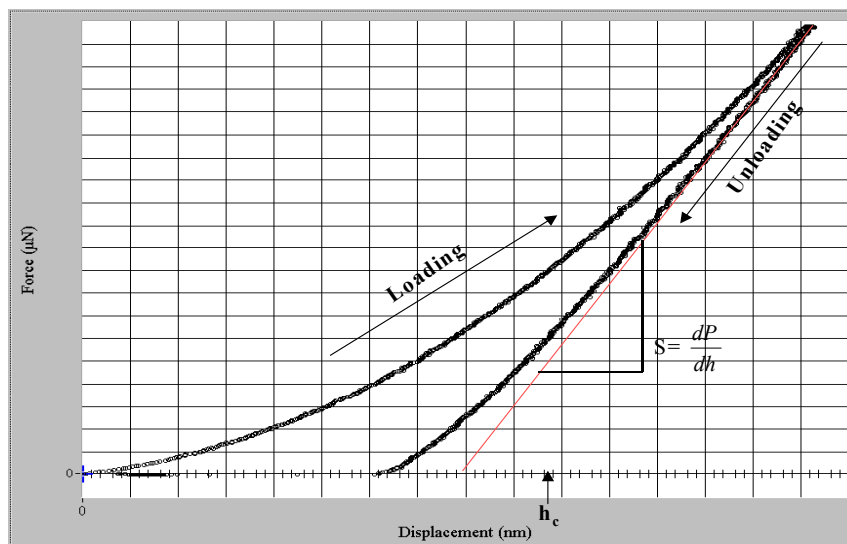


**Fig. 1. Loading and unloading curves and the definition of important parameter to estimate hardness and elasticity modulus**

**Rys.1. Krzywe obciążania i odciążania oraz definicja ważnych parametrów dla oceny twardości i modułu sprężystości**

The reduced modulus is defined by the following equation [20],  $E_r = S \frac{\sqrt{\pi}}{2\sqrt{A}}$ , where S is the unloading stiffness  $\left(\frac{dP}{dh}\right)$  and A is the projected contact area.

The reduced modulus is related to the modulus of elasticity (E) through the following equation,  $\frac{1}{E_r} = \frac{(1-\nu_1^2)}{E_1} + \frac{(1-\nu_2^2)}{E_2}$ , where the subscript 1 corresponds to the indenter material, the subscript 2 refers to the indented material, and  $\nu$  is Poisson's ratio. For a diamond indenter tip,  $E_1$  is 1140 GPa and  $\nu_1$  is 0.07. Poisson's ratio varies between 0 and  $\frac{1}{2}$  for most materials.

The unloading stiffness (S) is calculated by fitting the unloading curve to the power law relation,  $P = A(h - h_f)^m$ , where A,  $h_f$ , and m are arbitrary fitting parameters. The stiffness can be calculated from the derivative of the preceding equation:  $S = \frac{dP}{dh}(h_{\max}) = mA(h_{\max} - h_f)^{m-1}$ . The hardness is defined by the ratio of the maximum load to the projected contact area,  $H = \frac{P_{\max}}{A}$ .

The contact area is determined from a tip calibration function  $A(h_c)$  where  $h_c$ , the contact depth, is found by using the following equation:  $h_c = h_{\max} - \varepsilon \frac{P_{\max}}{S}$ . To account for edge effects, the deflection of the surface at the contact perimeter is estimated by taking the geometric constant  $\varepsilon$  as 0.75 [2,19].

## RESULTS AND DISCUSSION

The indentation load-displacement curves for TiN films are presented in Fig. 2. and the data for hardness and reduced elasticity modulus are given in Table 1.

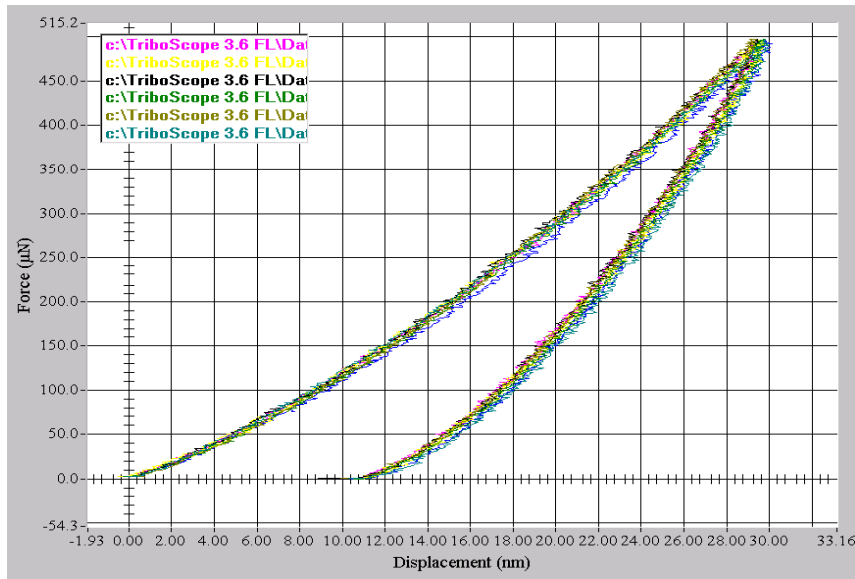


**Fig. 2. Load-displacement characteristics for TiN film**  
**Rys. 2. Charakterystyki obciążenie-odkształcenie dla warstwy TiN**

**Table 1. Hardness and reduced modulus for TiN/Si sample calculated on the basis of load-displacement curves shown in Fig. 2**

**Tablica 1. Twardość i zredukowany moduł sprężystości dla próbki TiN/Si obliczone na podstawie krzywych obciążenie-odciążenie pokazanych na rys. 2**

Indent #	Contact Depth [nm]	Reduced Modulus [GPa]	Hardness [GPa]
1	21.10	227.50	19.63
2	21.06	231.92	19.66
3	20.63	231.72	20.25
4	20.64	225.43	20.25
5	20.61	231.88	20.32
6	21.05	233.03	19.71
7	20.71	235.05	20.18
8	21.59	235.05	19.00
Average	20.92	231.45	19.88
Standard Deviation	0.34	3.40	0.46

In situ AFM images showed that the surface of the TiN/Si sample was very smooth. The load and unload parts of curve were very close and repeatable for all measurements. The same slope of these curves and the unloaded points (the top point of this curve) were almost the same – it changed in a small range. For this sample there was no high plastic deformation. We could estimate that fact from the area between load and unload curve. Area for these measurements wasn't very wide, so most of the deformation was elastic.

The load-displacement curves for CrN film are shown in Fig. 3, and their data of hardness and elasticity modulus are presented in Table 2.

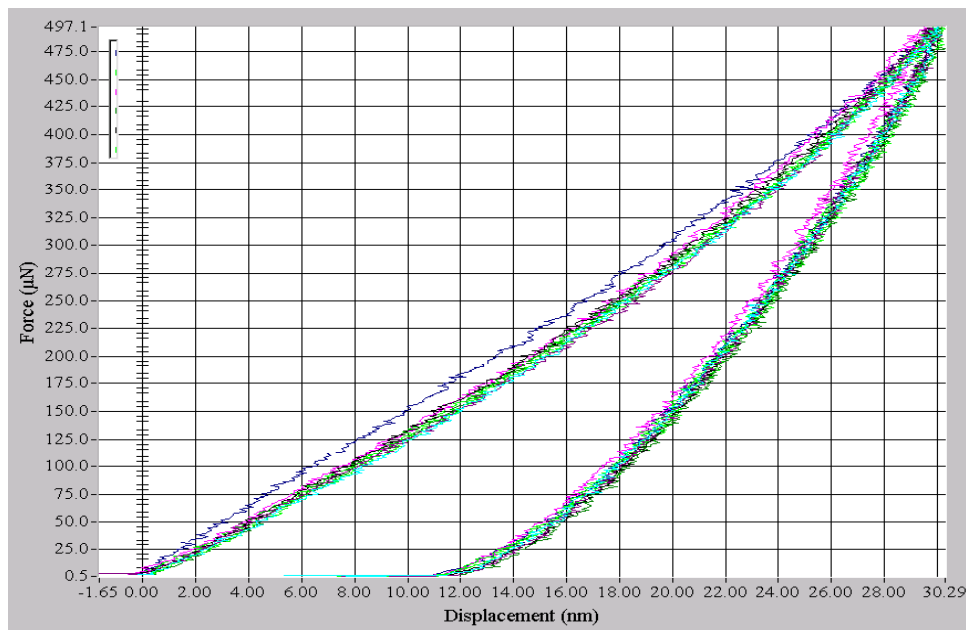


**Fig. 3. Load-displacement curves for CrN film**  
**Rys. 3. Krzywe obciążenie-odkształcenie dla warstwy CrN**

**Table 2. Hardness and elasticity modulus for sample CrN/Si**  
**Tablica 2. Twardość i moduł sprężystości dla próbki CrN/Si**

Indent #	Contact Depth [nm]	Reduced Modulus [Gpa]	Hardness [GPa]
1	20.94	221.53	19.82
2	21.35	221.38	19.32
3	20.74	232.67	20.06
4	21.57	227.71	19.01
5	21.15	225.18	19.56
6	21.13	226.35	19.60
7	21.28	228.78	19.40
8	21.10	221.58	19.64
Average	21.16	225.65	19.55
Standard Deviation	0.25	4.07	0.32

The similar to TiN film relatively uniform surface was observed for this sample. The plastic deformation was not distinct as results from the observation of the load-displacement curves.

The load-displacement curves for NbN film are presented in Fig. 4.

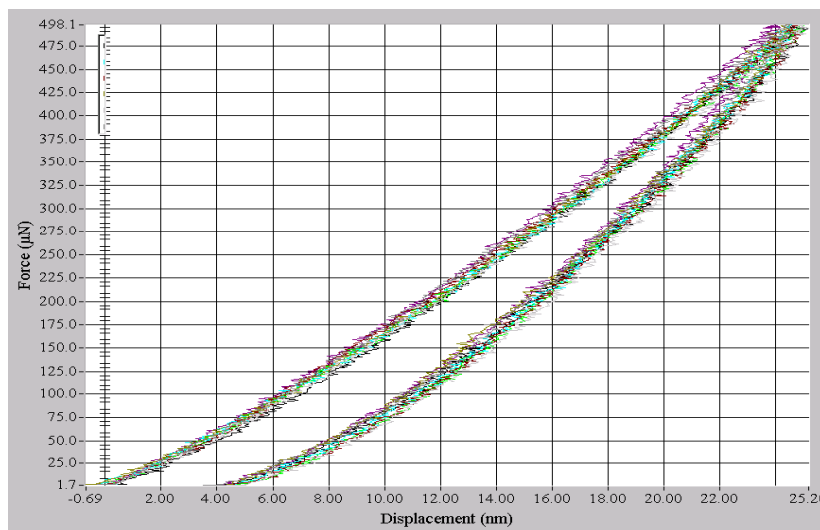


**Fig. 4. Load-displacement curves for NbN/Si sample**  
**Rys. 4. Krzywe obciążenie-odkształcenie dla próbki NbN/Si**

The results of the nanoindentations of NbN film are given in Table 3.

**Table 3. Summary of results from nanoindentation tests for NbN/Si sample**  
**Tablica 3. Podsumowanie wyników nanoindentacji dla próbki NbN/Si**

Indent #	Contact Depth [nm]	Reduced Modulus [GPa]	Hardness [GPa]
1	14.55	274.85	32.82
2	14.57	254.11	32.70
3	14.45	250.30	33.06
4	14.75	262.13	32.23
5	14.59	252.49	32.61
6	14.19	253.22	33.91
7	15.05	254.48	31.30
8	14.33	258.20	33.48
Average	14.56	257.47	32.76
Standard Deviation	0.26	7.92	0.79

The indentation load-displacement curves were used to estimate the hardness and elasticity modulus as a function of the depth of indentation. The comparison of these data for TiN, CrN and NbN films deposited on silicon are presented in Figs 5 and 6 respectively.



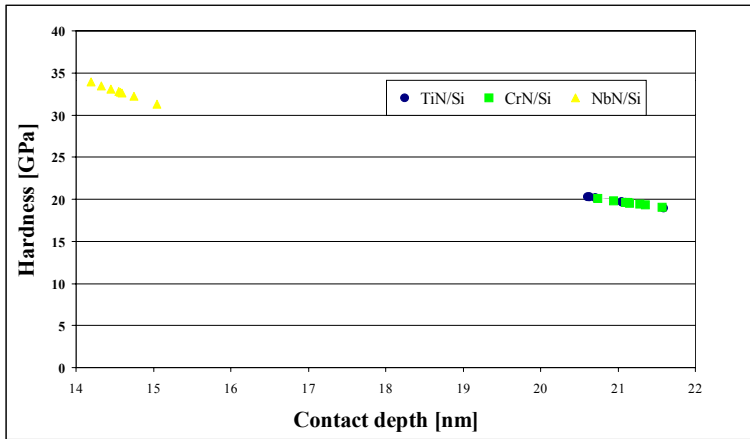


**Fig. 5. Comparison of hardness vs. indentation (contact) depth for TiN, CrN and NbN films**

**Rys. 5. Porównanie twardości w funkcji głębokości indentacji dla warstw TiN, CrN i NbN**

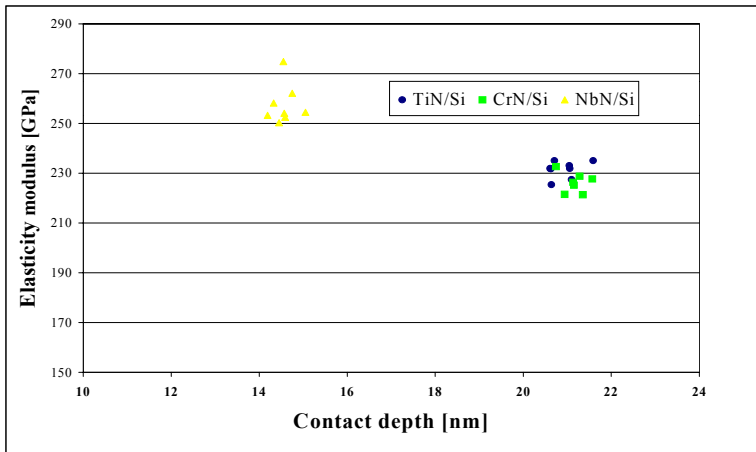


**Fig.6. Comparison of reduced elasticity modulus versus indentation (contact) depth for TiN, CrN and NbN films**

**Rys. 6. Porównanie zredukowanego modułu sprężystości jako funkcji głębokości indentacji dla warstw TiN, CrN i NbN**

The load-displacement curves for SiO<sub>2</sub>t (thermally deposited), SiO<sub>2</sub>p (plasma deposited) and Si<sub>3</sub>N<sub>4</sub> films are presented in Figs. 7, 8 and 9 respectively.

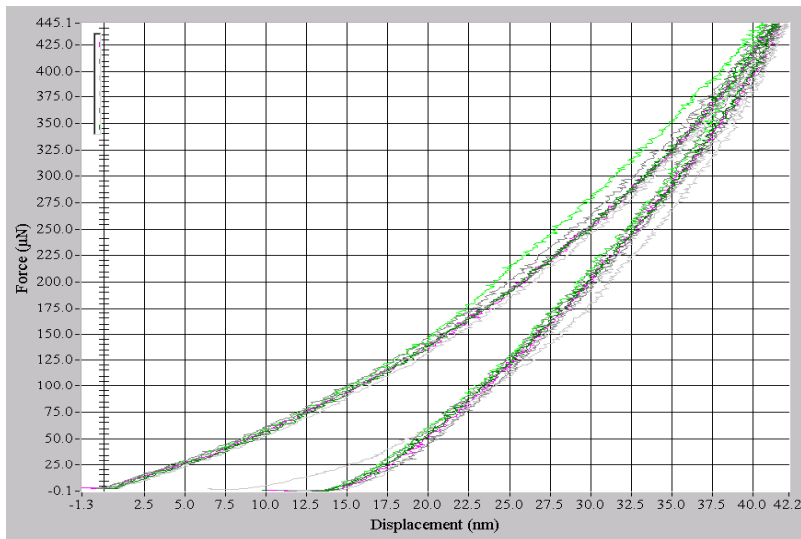


**Fig. 7. Load vs. displacement for SiO<sub>2</sub>t (thermally deposited) film**  
**Rys. 7. Krzywe obciążenie –odkształcenie dla warstwy SiO<sub>2</sub>t (osadzonej termicznie)**

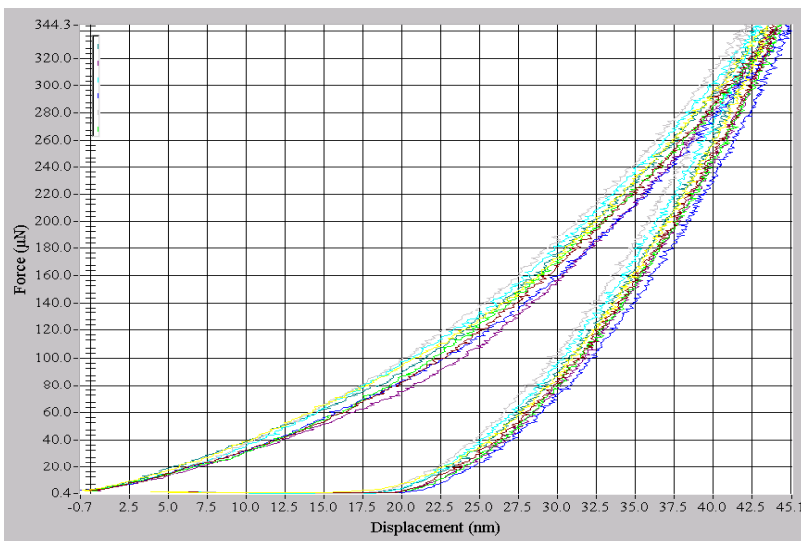


**Fig. 8. Load vs. displacement for SiO<sub>2</sub>p (plasma deposited) film**  
**Rys.8. Krzywe obciążenie-odkształcenie dla warstwy SiO<sub>2</sub>p (osadzonej plazmowo)**

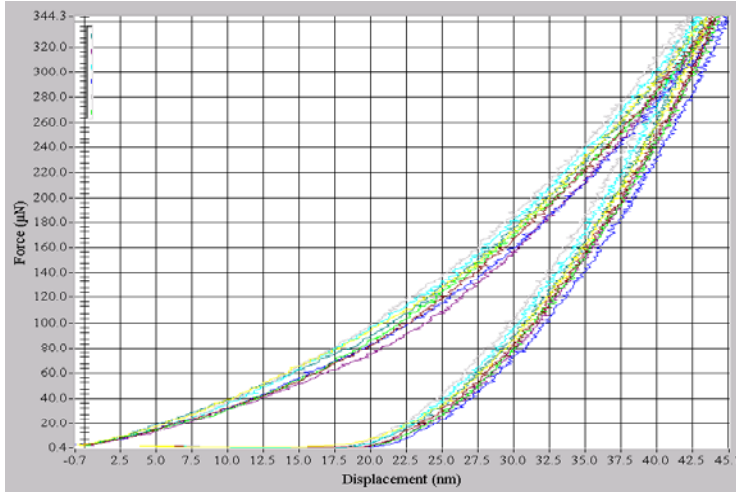


**Fig. 9. Load vs. displacement for  $\text{Si}_3\text{N}_4$  film**  
**Rys. 9. Krzywe obciążenie-odkształcenie dla warstwy  $\text{Si}_3\text{N}_4$**

The adequate hardness and elasticity modulus results are given summarised in Table 4.

Indent #	$\text{SiO}_2\text{t}$			$\text{SiO}_2\text{p}$			$\text{Si}_3\text{N}_4$		
	Contact Depth (nm)	Reduced Modulus (GPa)	Hardness (GPa)	Contact Depth (nm)	Reduced Modulus (GPa)	Hardness (GPa)	Contact Depth (nm)	Reduced Modulus (GPa)	Hardness (GPa)
1	27.43	111.05	12.02	33.01	97.29	7.03	24.97	162.96	16.91
2	27.78	107.30	11.77	33.63	94.16	6.83	25.00	159.88	16.89
3	27.32	103.29	12.07	32.42	97.97	7.23	24.83	159.39	17.03
4	27.18	107.84	12.17	34.27	92.52	6.64	25.20	161.76	16.68
5	30.23	116.57	10.38	31.95	101.69	7.40	25.32	161.46	16.56
6	27.78	102.30	11.78	33.50	92.54	6.88	25.59	159.57	16.30
7	27.78	103.75	11.80	33.30	92.98	6.94	25.15	165.37	16.74
8	27.49	104.92	11.97	33.01	95.58	7.02	24.84	162.09	17.05
Aver	27.87	107.13	11.74	33.14	95.59	7.00	25.11	161.56	16.77
Stand Deviat	0.98	4.77	0.57	0.72	3.24	0.23	0.26	2.01	0.25

**Table 4. Summary of results from indentation tests for microelectronic  $\text{SiO}_2\text{t}$  (thermally deposited),  $\text{SiO}_2\text{p}$  and  $\text{Si}_3\text{N}_4$  films**

**Tablica 4. Podsumowanie wyników indentacji dla warstw mikroelektronicznych  $\text{SiO}_2\text{t}$  (osadzonej termicznie),  $\text{SiO}_2\text{p}$  (osadzonej plazmowo) oraz  $\text{Si}_3\text{N}_4$ .**

From these characteristics it can be stated that the films, in particular  $\text{SiO}_2\text{t}$  (thermally deposited),  $\text{SiO}_2\text{p}$  (plasma deposited), deform elastically during the nanoindentation process.

The summarised data of hardness and elasticity modulus versus contact depth for the tested three microelectronic films are presented in Figs. 10 and 11 respectively.

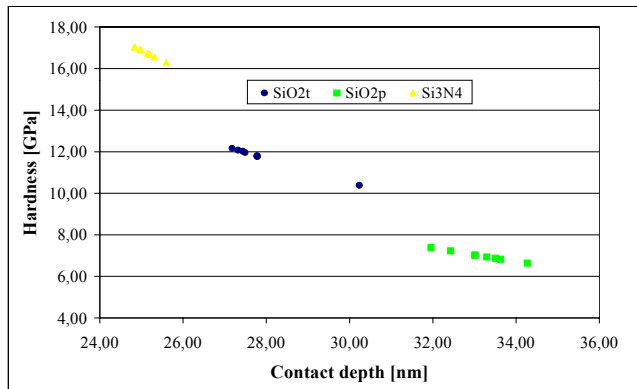


**Fig. 10. Hardness vs. contact depth for all three microelectronic films**  
**Rys.10. Twardość w funkcji głębokości indentacji dla wszystkich trzech warstw mikroelektronicznych**

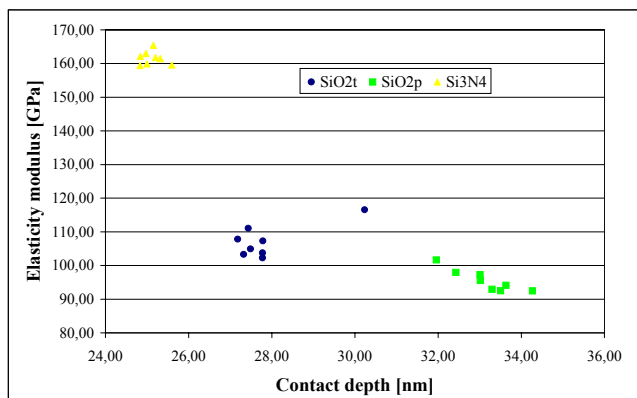


**Fig.11. Reduced modulus vs. contact depth for all three microelectronic films**  
**Rys.11. Zredukowany moduł sprężystości w funkcji głębokości indentacji dla wszystkich trzech warstw mikroelektronicznych**

The carried-out experiments showed that the mechanical properties of the tested films are different. The comparison of the hardness and elasticity modulus between TiN, CrN and NbN films demonstrated superiority of the

NbN film. However, the uniformity of the film looking for the distribution of its mechanical properties in the series of tests (as it can be stated from data given in Tables 1, 2 and 3) was found to be best for TiN film as contrast to NbN film. Since the mechanical properties depends on deposition technique, microstructure and chemical composition the differences between the tested films can result from the both last two reasons. The microstructural composition should has some effect on the uniformity of the film. In this case the best mechanical behaviour of NbN film could be attributed to the chemical bonds.

The mechanical properties of the microelectronic films differ significantly. The best mechanical properties demonstrated silicon nitride film. This is important founding since such films have been found to be interesting MEMS material in frictional tests [19]. The mechanical properties of plasma deposited silicon dioxide are poor as compared with silicon dioxide thermally deposited and silicon nitride.

The previous studies [21, 22] of the nanomechanical behaviour of various MEMS materials (single crystal silicon with different crystallographic orientation, polysilicon) showed that the hardness of silicon and elasticity modulus are around 9-11 GPa and 160-170 GPa, respectively. The tested silicon dioxide films are therefore not interesting materials to be used to perform some mechanical/tribological functions.

The comparison of the TiN, CrN and NbN films with  $\text{Si}_3\text{N}_4$  shows that the first three films behave better looking on demonstrated mechanical properties. Such films seems to be interesting coating materials and can be taken into consideration as potential candidates to perform mechanical/tribological functions in MEMS devices manufactured using silicon.

## CONCLUSIONS

Three ultrathin TiN, CrN and NbN films deposited by PVD technique on single crystal silicon wafer were tested using nanoindentation. The nanomechanical behaviour of these films was compared with the typical microelectronic films . The results of the investigation show that the best mechanical properties from TiN, CrN and NbN films demonstrated NbN film. The mechanical properties of two silicon dioxide films deposited by thermal or plasma process are poor as compared to silicon nitride film.

The mechanical properties of TiN, CrN, NbN and  $\text{Si}_3\text{N}_4$  are better than the mechanical properties of single crystal silicon used as substrate material. First three films were found to have higher hardness and elasticity modulus as compared to these properties of silicon nitride. Such films deposited on silicon can be considered as potential candidates to perform mechanical/tribological functions in the construction of MEMS devices.

## ACKNOWLEDGEMENTS

The authors are thankful for the State Committee for Scientific Research (KBN) for partial funding of these studies under the grant No. 7T11B 051 20. One of us (KM) is grateful for Hysitron Inc. for the possibility of training in the nanomechanical lab.

## REFERENCES

1. Bhushan B., Introduction to Tribology, J.Wiley, New York 2002
2. Bhushan B.(ed), Handbook of Micro/Nanotribology, 2<sup>nd</sup> ed., CRC Press, Boca Raton 1998
3. Bhushan B., Tribology and Mechanics of Magnetic Storage Devices, 2<sup>nd</sup> ed., Springer-Verlag, Berlin 1996
4. Bhushan B. (ed), Tribology Issues and Opportunities in MEMS, Kluwer Academic Publishers, Dordrecht 1998
5. Ludema K., Modeling and wear mechanisms, in: Fundamentals of Tribology and Bridging the Gap Between the Macro- and Micro/Nanoscale (B.Bhushan ed.), Kluwer Academic Publishers, Dordrecht 2001, 359-376
6. Bhushan B., Nanoscale tribophysics and tribomechanics, Wear 225-229 (1999) 465-492
7. Rabinowicz E., Friction and Wear of Materials, 2n ed., J.Wiley, New York 1995
8. Wei G., et al., Nanotribological studies of chromium thin films, Tribology Letters 13 (2002) 255-261
9. Burakowski T., Wierzchon T., Surface Engineering of Metals: Principles, Equipment, Technologies, CRC Press, Boca Raton 1998
10. Larsson M., et al., Mechanical and tribological properties of multilayered PVD TiN/NbN coatings, Surface Coatings Technology 86-87 (1996) 43-49
11. Martinez E., et al, Tribological performance of TiN supported molybdenum and tantalum carbide coatings in abrasion and sliding contact, Wear 253 (2002) 1182-1187
12. Hainsworth S.V., Soh W.C., The effect of the substrate on the mechanical properties of TiN coatings, Surface and Coatings Technology 163-164 (2003) 515-520
13. Lee J.W. et al., Mechanical property evaluation of cathodic arc plasma-deposited CrN thin films on Fe-Mn-Al-C alloys, Surface and Coatings Technology 168 (2003) 223-230
14. Tan J.N., Hsieh J.H., Deposition and characterization of (Nb,Cr)N thin films by unbalanced magnetron sputtering, Surface and Coatings Technology 167 (2003) 154-160

15. Martinez E., et al., Wear behavior of nanometric CrN/Cr multilayers, *Surface and Coatings Technology* 163-164 (2003) 571-577
16. Imbeni V., et al., Tribological behaviour of multi-layer PVD nitride coatings. *Wear* 251 (2001) 997-1002
17. Lu X.C. et al., Nanoindentation and microtribological behavior of Fe-N/Ti-N multilayers with different thickness of TiN layers, *Wear* 251 (2001) 1144-1149
18. Holmberg K., et al, A model for stresses, crack generation and fracture toughness calculation in scratched TiN-coated steel surfaces, *Wear* 254 (2003) 278-291
19. Fischer-Cripps A.C., *Nanoindentation*, Springer-Verlag, Berlin 2002
20. Oliver W.C., Pharr G.M., An improved technique for determining hardness and elastic modulus using load and depth sensing indentation experiments, *Journal of Materials Research* 7 (1992) 1564-1575
21. Rymuza Z. et al., Nanomechanical behaviour of silicon, *Tribologia* 30 (1999) No.3 397-409
22. Sundararajan S., Bhushan B., Micro/nanoscale tribology of MEMS materials, lubricants and devices, in: *Fundamentals of Tribology and Bridging the Gap Between the Macro- and Micro/Nanoscale* (B.Bhushan ed.), Kluwer Academic Publishers, Dordrecht 2001, 821-850

## **Nanomechaniczne zachowanie się ultracienkich warstw azotkowych osadzonych na krzemie**

### **Streszczenie**

Metodą nanoindentacji przeprowadzono badania ultracienkich warstw TiN, CrN i NbN osadzonych na płytce z krzemu krystalicznego celem oceny twardości i modułu sprężystości. Wyniki tych badań zostały porównane z wynikami podobnych prób dla mikroelektronicznych warstw dielektrycznych SiO<sub>2</sub> (dwa rodzaje – osadzane termicznie i plazmowo)) oraz Si<sub>3</sub>N<sub>4</sub>. Stwierdzone lepsze własności mechaniczne pierwszej grupy badanych warstw predestynują je do zastosowania jako warstwy ochronne na elementach mikrosystemów elektromechanicznych (MEMS).